AGU100 ADVANCING EARTH AND SPACE SCIENCE

Dear Author:

Thank you for publishing with AGU. Your proofs are attached. AGU and Wiley are committed to rapid posting of accepted papers. The accepted version of your paper is already available online (except for embargoed papers), providing visibility, and we strive to have final versions available within a few weeks. Following the guidelines for marking corrections and returning the proofs quickly will allow prompt online posting of the final version of your paper.

AGU Publications recently updated our style to follow leading practices in scholarly publishing, to simplify corrections and reduce copyediting changes. We are now following the APA style for grammar and markup. This style is used by many other journals and we hope that this change, over time, will lead to a simpler and standard experience for authors.

We have collected some information on how to increase the visibility of your paper here. Many of these steps can be taken after publication, so it is not too late to start. The online version of your paper includes "Altmetrics," which continually tracks and links to mentions in news outlets, Twitter, blogs, and other social media. A link to articles that cite your paper is also provided. Papers are also linked directly to any highlights provided by AGU and other similar AGU content. Recent highlights across AGU journals are collected here.

AGU is also, through Wiley, working to expand sharing of articles. Wiley piloted an initiative through the PDF reader Readcube that allows content to be shared freely to colleagues by authors and subscribers. This is now available for AGU content. For authors and subscribers, just click on the "share" link of your article in the Readcube reader. For the public and general reader, this service also allows free access to Wiley and thus AGU content from links in news stories.

Finally, your feedback is important to us. If you have questions or comments regarding your AGU Publications experience, including information on production and proofs, please contact us at publications@agu.org. We will also be contacting you soon after your article is published with an author survey. Please take a few minutes to respond to this online survey; your input is important in improving the overall editorial and production process. Thank you again for supporting AGU.

Sincerely,

Brooks Hanson
Sr. Vice President, Publications

2000 Florida Avenue, NW, Washington, DC 20009-1277
Tel: 202.462.6900
Fax: +1 202.328.0566
www.agu.org

WILEY

USING e-ANNOTATION TOOLS FOR ELECTRONIC PROOF CORRECTION

Required software to e-Annotate PDFs: Adobe Acrobat Professional or Adobe Reader (version 11 or above). (Note that this document uses screenshots from Adobe Reader DC.)
The latest version of Acrobat Reader can be downloaded for free at: http://get.adobe.com/reader/

Once you have Acrobat Reader open on your computer, click on the Comment tab (right-hand panel or under the Tools menu).

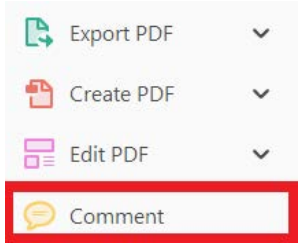

This will open up a ribbon panel at the top of the document. Using a tool will place a comment in the right-hand panel. The tools you will use for annotating your proof are shown below:

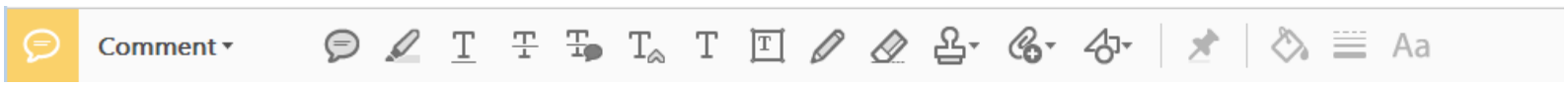

1. Replace (Ins) Tool – for replacing text.

Strikes a line through text and opens up a text box where replacement text can be entered.

How to use it:

- Highlight a word or sentence.
- Click on  .
- Type the replacement text into the blue box that appears.

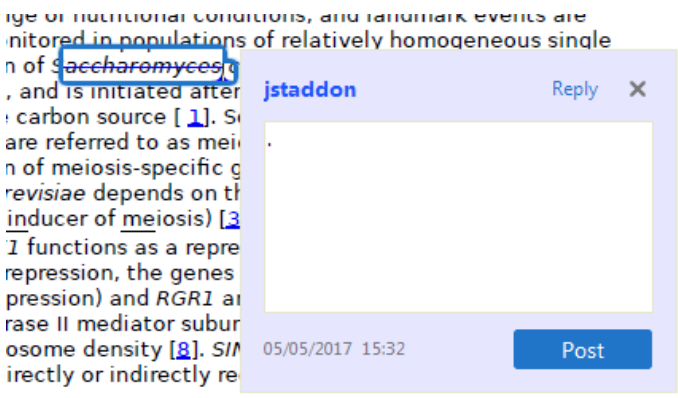

2. Strikethrough (Del) Tool – for deleting text.

Strikes a red line through text that is to be deleted.

How to use it:

- Highlight a word or sentence.
- Click on  .
- The text will be struck out in red.

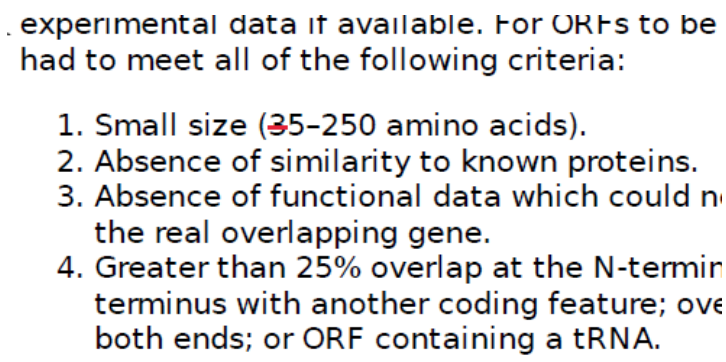

3. Commenting Tool – for highlighting a section to be changed to bold or italic or for general comments.

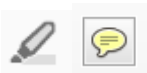

Use these 2 tools to highlight the text where a comment is then made.

How to use it:

- Click on  .
- Click and drag over the text you need to highlight for the comment you will add.
- Click on  .
- Click close to the text you just highlighted.
- Type any instructions regarding the text to be altered into the box that appears.

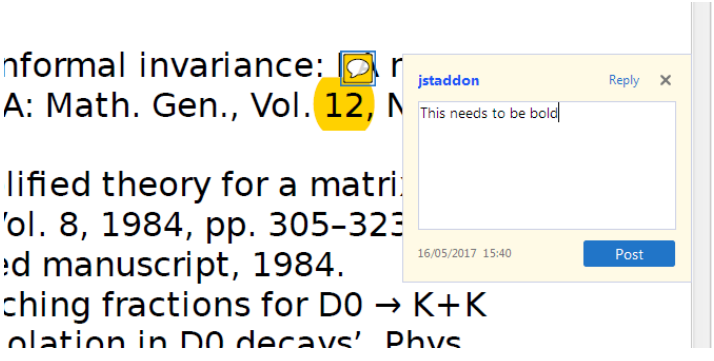

4. Insert Tool – for inserting missing text at specific points in the text.

Marks an insertion point in the text and opens up a text box where comments can be entered.

How to use it:

- Click on  .
- Click at the point in the proof where the comment should be inserted.
- Type the comment into the box that appears.

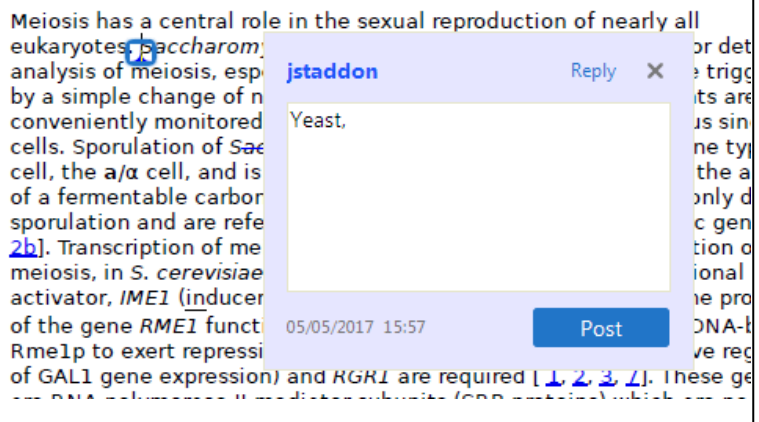

5. Attach File Tool – for inserting large amounts of text or replacement figures.

Inserts an icon linking to the attached file in the appropriate place in the text.

How to use it:

- Click on  .
- Click on the proof to where you'd like the attached file to be linked.
- Select the file to be attached from your computer or network.
- Select the colour and type of icon that will appear in the proof. Click OK.

  The attachment appears in the right-hand panel.

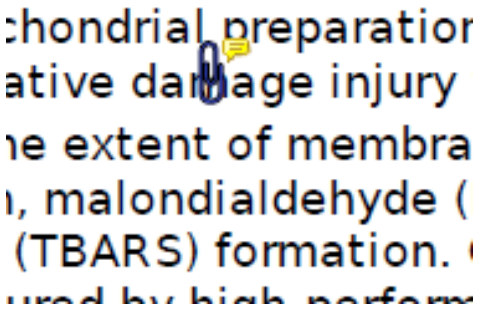

6. Add stamp Tool – for approving a proof if no corrections are required.

Inserts a selected stamp onto an appropriate place in the proof.

How to use it:

- Click on  .
- Select the stamp you want to use. (The Approved stamp is usually available directly in the menu that appears. Others are shown under *Dynamic*, *Sign Here*, *Standard Business*).
- Fill in any details and then click on the proof where you'd like the stamp to appear. (Where a proof is to be approved as it is, this would normally be on the first page).

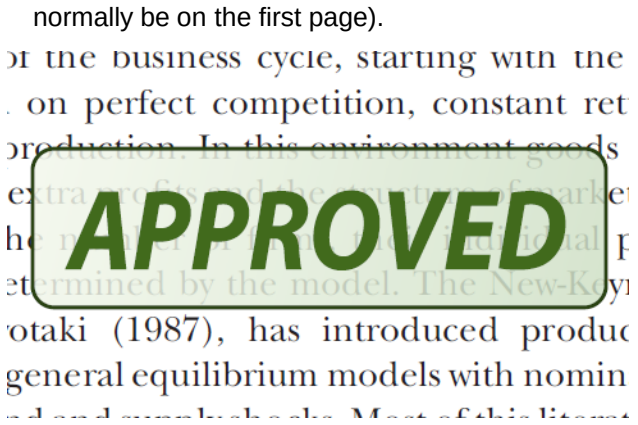

Drawing tools available on comment ribbon

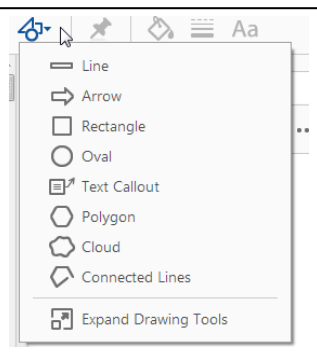

7. Drawing Markups Tools – for drawing shapes, lines, and freeform annotations on proofs and commenting on these marks.

Allows shapes, lines, and freeform annotations to be drawn on proofs and for comments to be made on these marks.

How to use it:

- Click on one of the shapes in the Drawing Markups section.
- Click on the proof at the relevant point and draw the selected shape with the cursor.
- To add a comment to the drawn shape, right-click on shape and select *Open Pop-up Note.*
- Type any text in the red box that appears.

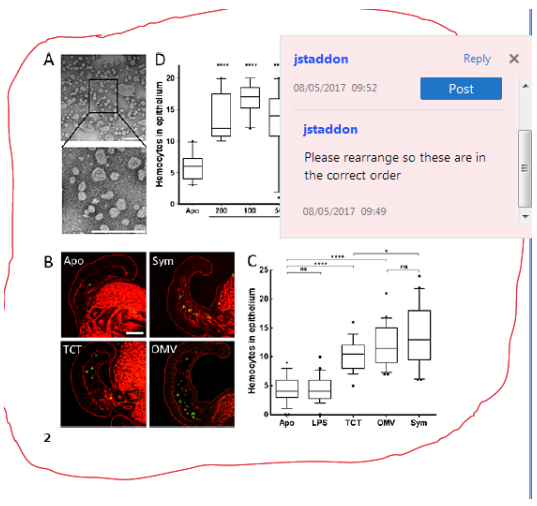

For further information on how to annotate proofs, click on the Help menu to reveal a list of further options:

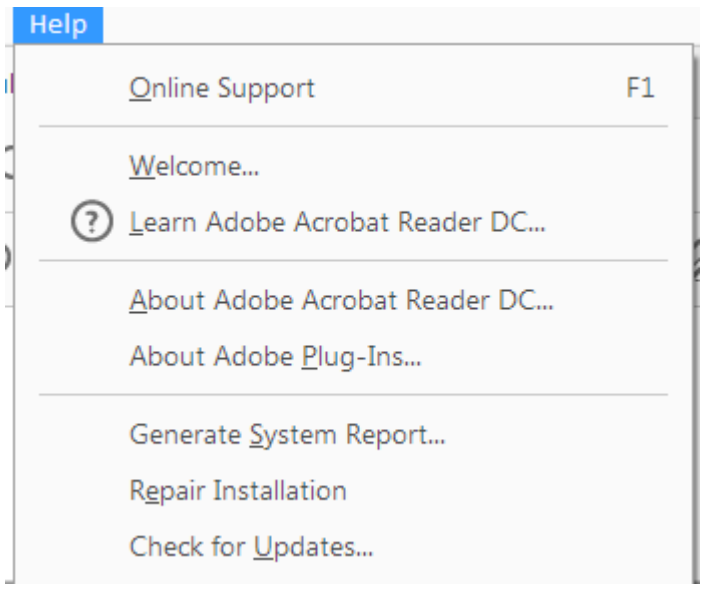

AGU100 ADVANCING EARTH AND SPACE SCIENCE

THIS IS NOT AN INVOICE

WILEY

GBC20797

PLEASE COMPLETE THE PUBLICATION FEE CONSENT FORM BELOW
AND
RETURN TO THE PRODUCTION EDITOR WITH YOUR PROOF CORRECTIONS

Please return this completed form and direct any questions to the Wiley Journal Production Editor at GBCprod@wiley.com.

To order OnlineOpen, you must complete the OnlineOpen order form at:
https://authorservices.wiley.com/bauthor/onlineopen_order.asp
Authors who select OnlineOpen will be charged the standard OnlineOpen fee for your journal, but excess publication fees will still apply, if applicable. **If your paper has generated excess publication fees, please complete and return the form below in addition to completing the OnlineOpen order form online (excess fees are billed separately)**. If you would like to choose OnlineOpen and you have not already submitted your order online, please do so now.

YOUR ARTICLE DETAILS

Journal: *Global Biogeochemical Cycles*
Article: Richardson, J. B., Aguirre, A. A., Buss, H. L., Toby O'Geen, A., Gu, X., Rempe, D. M., & Richter, D. d. B. (2018). Mercury sourcing and sequestration in weathering profiles at six Critical Zone Observatories. *Global Biogeochemical Cycles*, 32. https://doi.org/10.1029/2018GB005974

OnlineOpen: No **Words:** 6,778 **Tables:** 2 **Figures:** 3 **Total Publishing Units:** 19

Journal Base Fee:		$0
Excess Publishing Units:	0@$125	$0
Publication Fee Total:	USD	$0

Please provide the information requested below.

Bill to:

Name: _____

Institution: _____

Address: _____

Phone: _____ **Email:** _____

Signature: _____ **Date:** _____

An invoice will be mailed to the address you have provided once your edited article publishes online in its final format. Please include on this publication fee form any information that must be included on the invoice.

Publication Fees and Length Guidelines:
http://publications.agu.org/author-resource-center/

Frequently Asked Billing Questions:
http://onlinelibrary.wiley.com/journal/10.1002/(ISSN)2169-8996/homepage/billing_faqs.pdf

Purchase Order Instructions:
Wiley must be listed as the contractor on purchase orders to prevent delay in processing invoices and payments.

WILEY

Author Query Form

Journal: Global Biogeochemical Cycles

Article: gbc_20797

Dear Author,

During the copyediting of your paper, the following queries arose. Please respond to these by annotating your proofs with the necessary changes/additions.

- If you intend to annotate your proof electronically, please refer to the E-annotation guidelines.
- If you intend to annotate your proof by means of hard-copy mark-up, please use the standard proofing marks. If manually writing corrections on your proof and returning it by fax, do not write too close to the edge of the paper. Please remember that illegible mark-ups may delay publication.

Whether you opt for hard-copy or electronic annotation of your proofs, we recommend that you provide additional clarification of answers to queries by entering your answers on the query sheet, in addition to the text mark-up.

Query No.	Query	Remark
Q1	AUTHOR: Please fill out the Publication Fee Consent Form in these proofs (including complete mailing address) and return to the Production Editor with your proofs.	
Q2	AUTHOR: Please confirm that forenames/given names (blue) and surnames/family names (vermilion) have been identified correctly.	
Q3	AUTHOR: Please verify that the linked ORCID identifiers are correct for each author.	
Q4	AUTHOR: Supporting Information has been cited in the text but has not been supplied with the manuscript. Please forward the necessary files to the Production Editor so that they can appear online with your paper.	
Q5	AUTHOR: Please check that language changes made throughout this article are OK.	
Q6	AUTHOR: If this reference has now been published online, please add relevant year/DOI information. If this reference has now been published in print, please add relevant volume/issue/page/year information.	
Q7	AUTHOR: Ref. “Bazilevskaya et al., 2012” is cited in text but not provided in the reference list. Please provide details in the list or delete the citation from the text.	
Q8	AUTHOR: Ref. “St. Clair et al., 2015” is cited in text but not provided in the reference list. Please provide details in the list or delete the citation from the text.	
Q9	AUTHOR: Please provide volume number for ref. Andren and Nriagu (1979).	
Q10	AUTHOR: Please provide the chapter/article page numbers.	
Q11	AUTHOR: "Wang et al, 2013" has not been cited in the text. Please indicate where it should be cited; or delete from the Reference List.	

Please confirm that the funding sponsor list below was correctly extracted from your article: that it includes all funders and that the text has been matched to the correct FundRef Registry organization names. If a name was not found in the FundRef registry, it may not be the canonical name form, it may be a program name rather than an organization name, or it may be an organization not yet included in FundRef Registry. If you know of another name form or a parent organization name for a "not found" item on this list below, please share that information.

FundRef Name	**FundRef Organization Name**
National Science Foundation	National Science Foundation

SPi	Journal Code			Article ID					Dispatch: 29.08.18	CE: JAQA
	G	B	C	2	0	7	9	7	No. of Pages: 14	ME:

Revised proofs are sent only in the case of extensive corrections upon request

AGU100 ADVANCING EARTH AND SPACE SCIENCE

Global Biogeochemical Cycles

RESEARCH ARTICLE

10.1029/2018GB005974

Key Points:
- Mercury concentrations and inventories in weathering profiles were explored at six Critical Zone Observatories
- Using Hg/Ti ratios, we found that >88% of the Hg concentration was not rock-derived at Boulder Creek, Calhoun, and Southern Sierra CZOs
- Our study estimated that the top 10 m of regolith has Hg inventories two orders of magnitude greater than considered by current models

Supporting Information:
- Supporting Information S1
- Figure S1

Correspondence to:
J. B. Richardson,
soilbiogeochemist@gmail.com

Citation:
Richardson, J. B., Aguirre, A. A., Buss, H. L., Toby O'Geen, A., Gu, X., Rempe, D. M., & Richter, D. d. B. (2018). Mercury sourcing and sequestration in weathering profiles at six Critical Zone Observatories. *Global Biogeochemical Cycles*, *32*. https://doi.org/10.1029/2018GB005974

Received 2 MAY 2018
Accepted 13 AUG 2018
Accepted article online 21 AUG 2018

Mercury Sourcing and Sequestration in Weathering Profiles at Six Critical Zone Observatories

Justin B. Richardson[1,2], **Arnulfo A. Aguirre**[1], **Heather L. Buss**[3], **A. Toby O'Geen**[4], **Xin Gu**[5], **Daniella M. Rempe**[6], and **Daniel de B. Richter**[7]

[1]Department of Earth and Atmospheric Sciences, Cornell University, Ithaca, NY, USA, [2]Department of Geoscience, University of Massachusetts Amherst, Amherst, MA, USA, [3]School of Earth Sciences, University of Bristol, Bristol, UK, [4]Department of Land, Air and Water Resources, University of California, Davis, CA, USA, [5]Department of Geosciences, The Pennsylvania State University, University Park, PA, USA, [6]Department of Geosciences, Jackson School of Geosciences, University of Texas Austin, Austin, TX, USA, [7]University Program in Ecology and Nicholas School of Environment, Duke University, Durham, NC, USA

Abstract Mercury sequestration in regolith (soils + weathered bedrock) is an important ecosystem service of the critical zone. This has largely remained unexplored, due to the difficulty of sample collection and the assumption that Hg is predominantly sequestered within the surface soils (here we define as 0–0.3 m). We measured Hg concentrations and inventories in weathering profiles at six Critical Zone Observatories (CZOs): Boulder Creek in the Front Range of Colorado, Calhoun in the South Carolina Piedmont, Eel River in coastal northern California, Luquillo in the tropical montane forest of Puerto Rico, Shale Hills of the valley and ridges of central Pennsylvania, and Southern Sierra in the Sierra Nevada range of California. Surface soils had higher Hg concentrations than the deepest regolith samples, except for Eel River, which had lower Hg concentrations in surface soils compared to regolith. Using Ti normalization, CZOs with <12% rock-derived Hg (Boulder Creek, Calhoun, and Southern Sierra) had Hg peaks between 1.5 and 8.0 m in depth. At CZOs with >50% rock-derived Hg, Eel River Hg concentrations and pools were greatest at >4.0 m in the weathering profile, while Luquillo and Shale Hills had peaks at the surface that diminished within 1.0 cm of the surface. Hg and total organic C were only significantly correlated in regolith at Luquillo and Shale Hills CZOs, suggesting that Hg sorption to organic matter may be less dominant than clays or Fe(II) sulfides in deeper regolith. Our results demonstrate the importance of Hg sequestration in deep regolith, below typical soil sampling depths.

Plain Language Summary Our understanding of Hg cycling in the environment is built upon the assumption that surface soils are the most important in terrestrial ecosystems. Our study shows that weathered bedrock also plays an important role. The weathering of sedimentary rocks was the net sources of Hg, while the weathered igneous and metamorphic rocks were the net sinks for Hg. In addition, weathered bedrock holds far more Hg than soils, which is not taken into account in our current models.

1. Introduction

Hg is a toxic metal and global pollutant (Driscoll et al., 2013; Zahir et al., 2005). Chronic exposure to Hg can negatively impact humans (Holmes et al., 2009), aquatic organisms (e.g., Bloom, 1992; Harris et al., 2003) and terrestrial wildlife (e.g., Melgar et al., 2009; Richardson et al., 2015; Rimmer et al., 2005). Geochemical reservoirs, particularly terrestrial systems, sequester Hg, limiting its movement into terrestrial ecosystems and surface waters where it can bioaccumulate (Amos et al., 2013; Driscoll et al., 2007; Lamborg et al., 2002; Selin, 2009). The critical zone, the region from the top of vegetation down to the bottom of cycling ground water, is an important geochemical reservoir for Hg. Despite its importance, Hg sequestration in the regolith (including soil, unconsolidated rock, and weathered bedrock) of the critical zone has been poorly characterized, both for recent human and geologically derived Hg over kyr to Myr. Amos et al. (2013) estimated that soils and vegetation hold 12.1 Mg of Hg globally, and Andren and Nriagu (1979) approximated that deep mineral reservoirs (upper lithosphere such as bedrock and buried ocean sediments) hold 3×10^{11} Mg of Hg, which have accumulated over geologic time. Although mean residence time in deep mineral reservoirs has been estimated to be ~1 Gyr, Amos et al. (2013) note that deep mineral reservoirs may be released back to the atmosphere and terrestrial system through volcanic and anthropogenic emissions. As recently shown by Schuster et al. (2018), the large Hg reservoirs in soils, such as in the arctic

regions, could potentially alter the global Hg cycle. Moreover, deep regolith of the critical zone may be an important sink for Hg from weathering and geogenic Hg, in addition to more recent human emissions.

Hg in regolith may be substantially underestimated because most studies on the global Hg cycle focus on the top 0.3 to 0.5 m of the soil (e.g., Obrist et al., 2011; Richardson et al., 2013; Smith-Downey et al., 2010; Yu et al., 2014). Few studies have estimated the geochemical reservoir of Hg in deeper regolith and its contribution to the global Hg cycle (e.g., Andren & Nriagu, 1979). This is a serious drawback because total Hg in the oceans, atmosphere, soils, and vegetation are <0.01% of the estimated deep mineral reservoirs (Amos et al., 2013). Mercury accumulation in regolith of the critical zone has largely remained unexplored for two reasons: (1) difficulty in physical excavation of samples due to strenuous work and necessity of specialized equipment and (2) the assumption that most Hg cycling is sequestered within surface soils (here we define as 0–0.3 m). For example, the global Hg cycle model created by Smith-Downey et al. (2010) was developed using the top 0.3 m of soil. The few studies in tropical regions that sought to quantify deep regolith Hg found elevated concentrations below 1.0-m depth. Roulet et al. (1998) and Grimaldi et al. (2008) showed that soils in the tropics may have soil Hg concentrations of >100 ng/g at depths below 2.0 m. Moreover, Grimaldi et al. (2008) estimated that 75% to 90% of the elevated Hg within a 3.0-m-thick soil profile was from atmospheric sources. Thus, it is essential to understand the role of deep regolith on Hg sequestration to understand how deep regolith may serve as a sink.

Hg within regolith is sourced from geologic processes of weathering and background natural Hg deposition (Amos et al., 2013; Roulet et al., 1998) but more recently has been directly influenced from human industrial activities. Natural Hg emissions include volcanic activity and crustal degassing (Hylander & Meili, 2003; Nriagu & Becker, 2003; Pirrone et al., 2009). Anthropogenic Hg emissions include combustion of coal, industrial manufacturing, waste incineration, cement production, and mining activities (see Streets et al., 2017). As a result, Hg deposition has increased both regionally and globally since the 1800s (Pirrone et al., 2009; Selin, 2009; Streets et al., 2017). Streets et al. (2017) estimated that human activities are currently emitting Hg at 9.5×10^3 Mg/year and have added approximately 1.54×10^6 Mg from 1850 to 2010. Distinguishing between excess Hg, which is Hg added to regolith from atmospheric deposition or lateral transport and rock-derived Hg, sourced from in situ weathering of parent material, is key for determining if the critical zone is a net sink or source.

The objectives of this study were to determine the concentration and bulk inventories of Hg in weathering profiles of six upland Critical Zone Observatories (CZOs) and use geochemical normalization techniques to estimate sequestration of Hg not sourced from weathering of bedrock. Although we expected Hg concentrations to decrease with depth, we hypothesized that Hg inventories in deep regolith (>1.0 m) would be equal to or greater than Hg in surface soils (0–0.3 m) due to the greater mass and depth of material. Moreover, we anticipated that the majority of Hg inventories would not be sourced from weathering but instead sourced from atmospheric deposition or lateral transport of geogenic or anthropogenic Hg (from weathering of bedrock; e.g., Grimaldi et al., 2008; Guedron et al., 2006; Hissler & Probst, 2006; Zhang et al., 2015). By estimating the deeper accumulation of Hg, we aimed to test if the biogeochemical cycle for terrestrial Hg should include Q5 deep regolith inventories.

2. Materials and Methods

2.1. Critical Zone Observatories

2.1.1. Boulder Creek CZO

Boulder Creek CZO is located in the front range of the Rocky Mountains, within the Boulder Creek watershed, in north central Colorado, USA. Eight samples of regolith profile were collected over a 7.0-m depth from Gordon Gulch watershed, which is situated in Arapahoe National Forest. The lithology is dominated by biotite gneiss and is forested with evergreen vegetation, primarily lodgepole pine (*Pinus contorta*) and ponderosa pine (*Pinus ponderosa*). Gordon Gulch is considered a montane-steppe climate, with the majority of precipitation during spring and with lowest precipitation amounts in winter. Additional climatic and spatial information is given in Table 1. Samples were collected by borehole drilling in June 2014. T1

2.1.2. Calhoun CZO

Calhoun CZO is located in the Southern Piedmont in South Carolina, within the US Forest Service's Calhoun Experimental Forest, a 2,057-ha area that for nearly 70 years has been the site of studies of land and water

Table 1
Ecosystem and Geologic Properties of Sampling Sites at the Six Critical Zone Observatories

Study area		Mean elevation (m a. s.l.)	Latitude	Longitude	MAT (°C)	MAP (mm/year)	Vegetation	Soil	Bedrock
Boulder Creek CZO	Gordon gulch watershed	2,716	40°01′09″N	105°28′39″W	4	735	Evergreen forest	Inceptisols	granite-gneiss
Calhoun CZO	Research Area 1	124	34°36′23.6″N	81°43′24.8″W	16	1,250	Pine hardwood	Ultisols	granitic gneiss
Eel River CZO	Rivendell	455	39°43′46″N	123°38′39″W	12	2,150	Mixed evergreen	Alfisols	argillite
Luquillo CZO	Rio Icacos watershed - Guaba Ridge	680	18°17′02″N	65°47′20″W	21	4,200	Tropical forest	Inceptisols	quartz diorite
Shale Hills CZO	Susquehanna Shale Hills Catchment	280	40°39′52″N	77°54′22″W	10	1,050	Northern hardwoods	Inceptisols-Ultisols	shale
Southern Sierra CZO	Providence Creek P301	1,250	37°03′36″N	119°11′27″W	9	1,100	Coniferous	Inceptisols	granodiorite

Note. MAT = mean annual temperature, MAP = mean annual precipitation.

degradation and forest regeneration caused by agricultural land uses and reforestation (Richter & Markewitz, 2001). The Calhoun CZO has low to moderately steep hills, which are derived from granitic-gneiss, and a subtropical climatic zone. Vegetation is dominated by loblolly pine (*Pinus taeda*) and mixed hardwoods primarily oak (*Quercus* spp) and hickory (*Carya* spp; Richter & Markewitz, 2001). Fourteen subsamples of weathering profile were obtained in 2016 from a depth 0 to 12.2 m. Details of the collection and processing of geoprobe and drill core samples can be found in Bacon et al. (2012). In brief, soil samples (0–6.0 m) were collected from three cores of soil, and saprolite and deep saprolite (6.1–18.3 m) were sampled with a three-wing auger bit. Samples were crushed, sieved to <2 mm, and air-dried. Samples from the 18.3-m depth were considered representative of the parent rock Hg concentrations.

2.1.3. Luquillo CZO

The Luquillo CZO is located in the El Yunque National Forest, in northeastern Puerto Rico. Luquillo CZO began as the Luquillo Experimental Forest and also has been studied as a Long-Term Ecological Research site and a United States Geological Survey Water, Energy, and Biogeochemical Budgets site. Luquillo CZO is a tropical montane forest and has an average temperature of 21 °C (Murphy et al., 2012). Precipitation increases with elevation from 2,500 to 4,500 mm/year (Garcia-Martino et al., 1996), with about 4,200 mm/year reaching the Guaba ridge study site (about 680 m a.s.l. in the Rio Icacos watershed) and strong topographical variations (Murphy et al., 2017). Vegetation consists of *Dacryodes excelsa*, *Prestoea montana*, *Sloanea berteroana*, *Cordia borinquensis*, *Manilkara bidentata*, *Schefflera morototoni*, *Cecropia schreberiana*, *Micropholis garciniifolia*, *Henriettea squamulosa*, and *Quararibea turbinate* (Weaver & Gould, 2013). Soils, which were Inceptisols, were sampled (from 0 to 1.72 m) from site LG1 on the Guaba Ridge (Buss et al., 2017; White et al., 1998) in February 2017. Deeper regolith samples were taken in 2010 from archived material from site LG1 (Buss et al., 2005, 2017) and borehole LGW1 (Buss & White, 2012; Orlando et al., 2016), near the Guaba Ridge. In total, 11 regolith samples over 15.9 m in depth were analyzed.

2.1.4. Southern Sierra CZO

The Southern Sierra CZO is located in Fresno County, CA, USA, within the Kings River Experimental Watershed, a long-term research site established by the Pacific Southwest Research Station of the US Forest Service (Hunsaker & Eagan, 2003). Southern Sierra CZO lies outside the limits of recent glaciation, in a sequence of range-parallel ridges and valleys, with alternating steep and gentle terrain of granitic bedrock. We focused on P301, the head of Providence Creek, which has a montane-steppe climate. Vegetation is dominated by a mixed coniferous forest consisting of *Abies concolor*, *P. ponderosa*, *Pinus jeffreyi*, *Quercus kelloggii*, *Pinus lambertiana*, and *Calocedrus decurrens*, with intermixed chaparral. Eleven samples from 0 to 11.0 m in depth were collected in 2011, using a Geoprobe®. For more information regarding sample collection and processing, please see (Holbrook et al., 2014).

2.1.5. Eel River CZO

The Eel River CZO is located in Mendocino County, CA, USA, and lies within the Northern California Coast Ranges. Samples were collected from the Rivendell hillslope within the Elder Creek watershed in the

Angelo Coast Range Reserve. The bedrock consists of Franciscan argillites and turbidite deposits, which were accreted and uplifted during subduction of the Pacific Plate under the North American Plate. The Eel River is characterized by steep topography with active uplift and channel incision, at rates of 0.2–0.4 mm/year (Fuller et al., 2009), and deep-seated landsliding. The climate is generalized as coastal Mediterranean with a mean 2,156 mm/year of precipitation and 11.6 °C. Vegetation is dominated by a mixed evergreen forest including *Pseudostuga menziesii*, *Quercus wislizeni*, *Notholithocarpus densiflorus*, *Arbutus menziesii*, *Sequoia sempervirens*, and *Umbellularia californica*. Samples were collected at the Rivendell site within the Eel River CZO via auguring using a track-mounted rig. Augured samples were recovered and aggregated approximately every 0.76 m (2.5 ft) over a 16.31-m depth. Within each 0.76-m interval, subsamples were collected, bagged, and labeled with depth ranges. To determine the bulk density of the bedrock, bedrock fragments (approximately 1.5–3.5 g) were recovered by hand from depth intervals greater than 5 m. Rock fragments were weighed and measured for their total (envelope) volume using a Micromeretics Geopyc 1360 envelope density analyzer.

2.1.6. Shale Hills CZO

The Shale Hills CZO is located in Huntingdon County, PA, USA. Shale Hills CZO are just south outside the southern extent of recent glaciation, in a sequence of range-parallel ridges and valleys, with alternating steep and gentle terrain of silurian Rose Hill shale. The climate at Shale Hills CZO is considered temperate, with precipitation averages of 1,070 mm/year with mean annual temperatures of 10 °C. Vegetation at Shale Hills CZO is northern hardwoods with interspersed conifers, dominated by *Quercus* spp., *Carya* spp., *Pinus* spp., *Tsuga canadensis*, and *Acer rubrum*. The borehole (CZMW8) was drilled under the southern ridge. The air-dried core samples were pulverized using a mortar and pestle to pass through a 100-mesh sieve (<150 μm). Further information on the collection and processing of borehole core samples can be found in Jin et al. (2010). Concentrations of major elements and total carbon of the samples were published in Sullivan et al. (2016).

2.2. Total Element Quantification

Total Hg concentrations for regolith subsamples were quantified using a Direct Mercury Analyzer-80 (Milestone Inc.). Subsamples were oven-dried to a constant weight at approximately ~70 °C, which has been shown to release up to 8% of the total Hg but typically releases <3% (Hojdová et al., 2015). For the Hg measurement, 100 ± 10 mg of finely ground and homogenized subsamples were weighed into steel boats and ashed at 650 °C, trapping Hg on gold amalgam. The gold amalgam is heated to 850 °C, and Hg is quantified by an atomic absorption spectrophotometer. To ensure quality, every 15 samples included a duplicate and a preparation blank. Montana soil SRM 2711a was used as a standard reference material (SRM; National Institute of Standards and Technology, Gaithersburg, MD, USA). Preparation blanks were below detection limits (<0.05 ng/g), and duplicate variations were within 5%. SRM Hg measurements were always within 10% of their certified values. Total Hg values for each horizon are given in supporting information Table S1.

Subsamples of regolith from the six CZOs were prepared for geochemical analyses for Ti first by drying to a constant weight at 105 °C. Samples were then pulverized in a boron carbide mortar and pestle to <100 μm. For total sample digestion, 2 ml of 25 M HF acid and 5 ml of distilled 16 M HNO_3 (Trace metal grade, VWR Analytical, Radnor, PA, USA) were added to a 100-mg subsample and heated to 95 °C in sealed 30-ml Teflon PFA vials. After complete digestion of visible materials, samples were dried to a powder and redissolved in 0.5 M HNO_3. Regolith digests were diluted with deionized water and analyzed for trace metals with an Element 2 ICP-MS (Thermo-Scientific, Waltham, MA, USA). With every 20 samples, we included at least one preparation blank, a duplicate, and an SRM. W-2 diabase and G-2 granite from the United States Geological Survey were used as SRMs for regolith samples. Recoveries for total digests of Ti were 82–104% of certified values. The variation between intrasample duplicates was <7%, and Ti concentrations in the preparation blank samples were <0.01 μg/g.

Soil carbon data were obtained for each CZO: Calhoun (Bacon et al., 2012; Fimmen et al., 2008), Eel River (Druhan et al., 2017), Luquillo (Buss et al., 2005), and Southern Sierra (O'Geen, in prep). Total organic C Q6 (TOC) concentrations in soil and regolith samples were measured for Boulder Creek and Shale Hills CZO samples using the Carlo-Erba NA 1500 Element Analyzer (Thermo Scientific, Waltham, MA, USA). In brief, 6 ± 1-mg subsamples, ground to <0.5 mm, were combusted. Every 20 samples included one blank, one atropine SRM, and a duplicate. Limits of quantification for the Carlo-Erba NA 1500 Element Analyzer was 0.02%. TOC concentrations in Atropine SRMs were with 3% of its certified value and <10% relative percent difference.

Because soil samples were acidic soils, the contribution of C from calcium carbonates was presumed to be negligible.

2.3. Quantifying Rock-Derived and Excess Hg

We applied a normalization ratio of Hg/Ti, similar to mass balance coefficient analyses, to identify Hg sourced from bedrock weathering and additions to the weathering profiles from external sources, that is, atmospheric deposition or lateral transport (Brimhall & Dietrich, 1987; Oh & Richter, 2005; Zhang et al., 2015). Mercury was referenced to Ti in the deepest weathered bedrock samples in each regolith profile (Grimaldi et al., 2008; Guedron et al., 2006; Zhang et al., 2015). Although Ti is known to be more mobile than Zr during weathering, Ti exists in higher concentrations and avoids errors associated with anomalies in zircon crystal abundance and incomplete zircon digestion. For each depth sample in the regolith profile, the concentrations of $Hg_{rock\text{-}derived}$ and Hg_{excess} were estimated by normalizing Hg concentrations to Ti concentrations (Grimaldi et al., 2008; Guedron et al., 2006; Hissler & Probst, 2006). This method assumes that the element Ti contained in the parental material undergoes similar pedogenic processes as Hg, and $Hg_{rock\text{-}derived}$ is the fraction of Hg within the regolith sourced from weathering of parent material. Hg not accounted for as $Hg_{rock\text{-}derived}$ is assumed to be Hg_{excess}, which is assumed to be sourced from atmospheric deposition of natural and anthropogenic processes or laterally transported to the regolith. We calculated a theoretical Hg concentration [$Hg_{rock\text{-}derived}$] for each depth using the deepest, least weathered sample for each weathering profile using the following equation (1) (Grimaldi et al., 2008; Guedron et al., 2006):

$$[Hg_{rock-dervied}]_s = \frac{[Hg_p]}{[Ti_p]} \times [Ti_s] \quad (1)$$

where the subscripts refer to each depth of the profile and the subscript p refers to the least weathered bedrock. The extent of the weathering was visually confirmed using light microscopy, Al, Fe, Ti, and Zr ratios (Al, Fe, and Zr data not presented), and previous studies at each CZO.

2.4. Hg Inventory Calculation and Data Analyses

Using $Hg_{rock\text{-}derived}$ concentrations, Hg_{excess} concentrations, bulk density data, and measured depths, we calculated the storage of Hg inventories in each CZO weathering profile. To calculate Hg inventories, Hg concentrations were multiplied by bulk density measurements from either the samples themselves or from other samples at the same depth at the same CZO. Hg concentrations were assumed to be representative of their depth and used to create a continuous estimate of Hg mg/m^3 from 0 to 10 m depth. For Boulder Creek CZO, which was only sampled to the 7-m depth, the final sample was extrapolated down to the 10-m depth, assuming bulk density and Hg concentrations remained constant to the 10-m depth. The continuous Hg estimates were then split into four depth intervals: 0–0.3, 0.3–1.0, 1.0–4.0, and 4.0–10.0 m.

We tested the association of Hg, Hg_{excess}, and $Hg_{rock\text{-}derived}$ with TOC using linear regressions for each CZO and with generalized linear mixed model regressions with each CZO as a random effect. All regressions were performed using MATLAB (MATLAB 2016, Mathworks, Natick, MA, USA). For Hg concentrations and inventories, error bars were measurement errors based upon coefficients of variations for the samples.

3. Results

3.1. Mercury Concentration Profiles

Hg concentrations in weathering profiles across the six CZOs ranged from 0.4 to 281 ng/g with an average of 47 ng/g and median of 16 ng/g (Figure 1; supporting information Table S1). Comparing Hg across CZOs, Hg concentrations throughout the weathering profiles were lowest at Boulder Creek CZO and highest in Eel River CZO regolith (Figure 1). Highest Hg concentrations occurred in surface soils for weathering profiles at Luquillo, Shale Hills, and Southern Sierra CZOs (Figure 1). Boulder Creek, Calhoun, and Eel River CZOs had highest Hg concentration peaks deeper in weathering profile (Figure 1). Mercury concentrations were higher between the 1.8- and the 4.0-m depth for Boulder Creek, Calhoun, Luquillo, and Southern Sierra CZOs and at the 6.30-m depth for Eel River CZO.

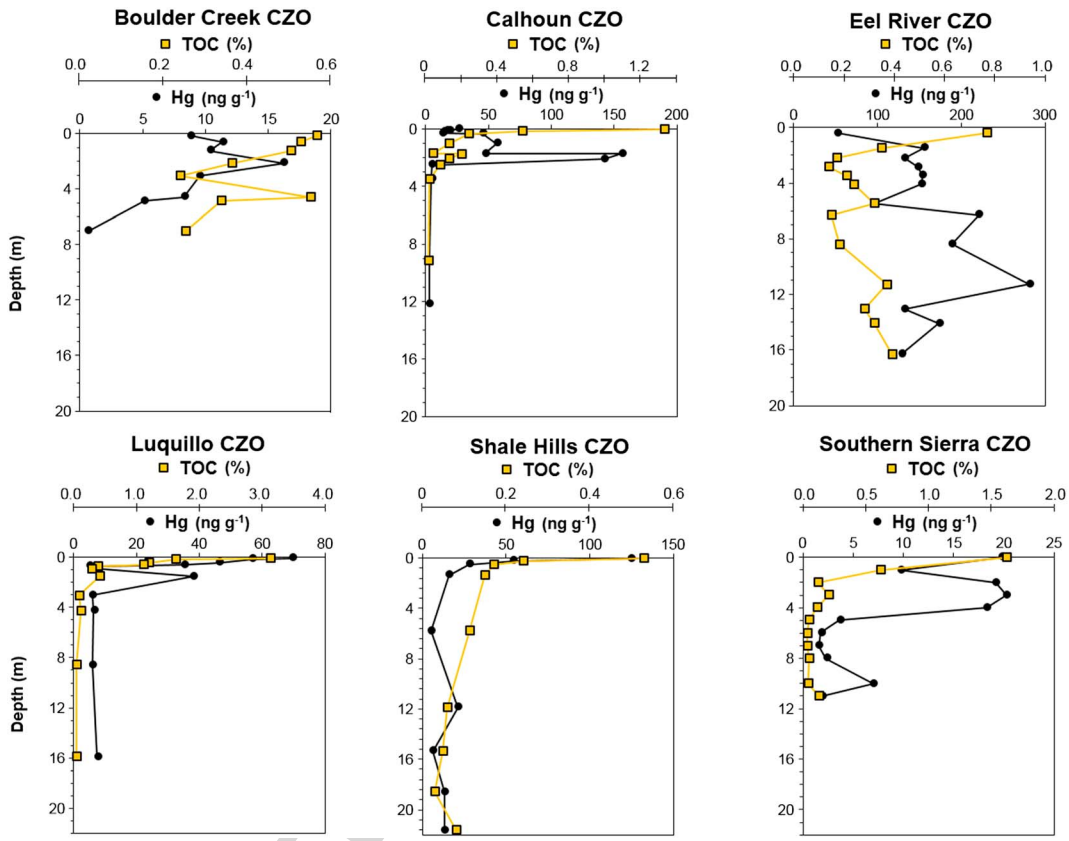

Figure 1. Total Hg concentrations (ng/g) in weathering profiles for the six Critical Zone Observatories (CZOs). Please note that Hg concentration scales (*x* axis) are not the same.

3.2. Excess and Rock-Derived Hg Concentrations

Most of the Hg was Hg_{excess} in the top 4.0 m at CZOs dominated with igneous and metamorphic bedrocks (Boulder Creek CZO, Calhoun CZO, Luquillo CZO, and Southern Sierra CZO; Figure 2). At Boulder Creek and Calhoun CZOs, Hg_{excess} was >88% of the Hg throughout the majority of the profile. At Southern Sierra CZO, Hg_{excess} was >86% of the Hg for the top 4 m but decreased to <5% between 5.0 and 11.0 m. Luquillo CZO showed that Hg_{excess} was the dominant Hg fraction at >80% of the Hg concentration for the top 0.6 m but dropped to <5% Hg_{excess} below 4.0 m (Figure 2). Eel River and Shale Hills CZOs, which had regolith derived from sedimentary rocks, had higher Hg concentrations and were dominated by $Hg_{rock\text{-}derived}$ for most of their weathering profiles, except in the top 0.5 m at Shale Hills CZO

3.3. Mercury Inventories

Hg inventories for the top 10.0 m were similar across most CZOs, ranging from 117 to 226 mg/m^2 (supporting information Table S2), except for Eel River CZO (3,753 mg/m^2). Hg inventories in the 0–0.3-m depth interval were comparable across CZOs, ranging between 6.2 mg/m^2 at Boulder Creek CZO and 31 mg/m^2 at Calhoun CZO. Hg inventories in the 0.3–1.0-m depth interval were also comparable across CZOs, ranging between 20 mg/m^2 at Boulder Creek and Shale Hills CZOs and 88 mg/m^2 at Eel River CZO. However, 1.0–4.0- and 4.0–10.00-m depth intervals were similar for all CZOs ranging between 22 and 158 mg/m^2 except for Eel River CZO, which had 918 and 2,589 mg/m^2 for the 1.0–4.0 and 4.0–10.0 m depth intervals, respectively. Considering Hg inventories normalized to their depth interval, the mg/m^3 was comparable across CZOs (21–103 mg/m^3) and decreased with depth except for Eel River CZO, which had increasing Hg inventories with depth (40 mg/m^3 at 0–0.3 m to 586 mg/m^3; data not shown). Although Hg inventories normalized to depth interval decreased deeper in the profile, Hg inventories deeper in the regolith profile were much larger than in the 0–0.3-m surface soils.

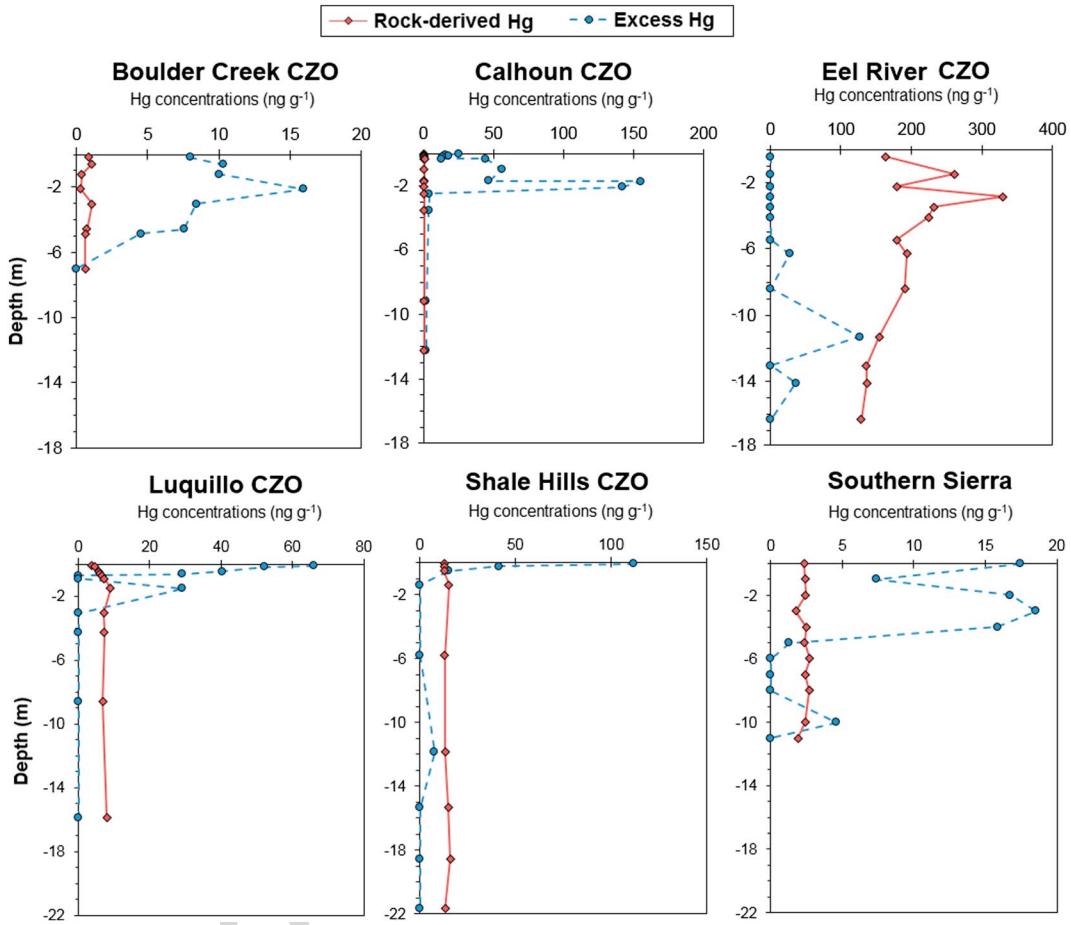

Figure 2. Profiles of $Hg_{rock\text{-}derived}$ and Hg_{excess} concentrations for the six Critical Zone Observatories (CZOs) using equation (1).

$Hg_{rock\text{-}derived}$ inventories in the top 10.0 m of regolith ranged substantially across CZOs in size, over two orders of magnitude, and in percent of the Hg inventory, ranged from 5% to 81% of the Hg inventories. CZOs with the lowest $Hg_{rock\text{-}derived}$ inventories in the top 10.0 m were Boulder Creek (10 mg/m^2 or 9%), Calhoun (11 mg/m^2 or 5%), and Southern Sierra (32 mg/m^2 or 22%). CZOs with the highest $Hg_{rock\text{-}derived}$ fractions in the top 10.0 m inventories were Luquillo (135 mg/m^2 or 60%), Shale Hills (123 mg/m^2 or 57%) and Eel River (2,816 mg/m^2 or 75%; supporting information Table S2). Greater than 85% of the Hg inventory in the 0.3–1.0-m depth interval was Hg_{excess} at Boulder Creek CZO, Calhoun CZO, and Southern Sierra CZO. However, only 53% of Hg in the 0.3–1.0-m depth interval at Luquillo CZO was Hg_{excess} (Figure 3). The F3 1.0–4.0-m depth interval had the greatest total Hg inventories, ranging from 69 mg/m^2 at Boulder Creek CZO to 88 mg/m^2 at Calhoun CZO. Of the Hg in the 0.3–1.0-m depth interval, >88% was Hg_{excess} at Boulder Creek CZO, Calhoun CZO, and Southern Sierra CZO. However, the 1.0–4.0-m depth interval at Luquillo CZO had only 32% Hg_{excess}.

3.4. Mercury Concentrations With TOC

Using linear regressions, Hg concentrations were significantly and positively correlated with TOC at Luquillo CZO (R = 0.91) and Shale Hills (R = 0.96) but not at Boulder Creek (R = 0.34), Calhoun CZO (R = −0.23), Southern Sierra (R = 0.48), or Eel River (R = −0.02) CZOs (Table 2; supporting information Figure S1). T2 Similarly, Hg_{excess} was significantly correlated with TOC at Luquillo and Shale Hills CZO (Table 2). $Hg_{rock\text{-}derived}$ was only significantly correlated with TOC at Luquillo, negatively (Table 2). Overall, there was no significant correlation between any of the three Hg concentrations with TOC across all CZOs, using generalized linear mixed model regressions with CZOs as a random effect variable.

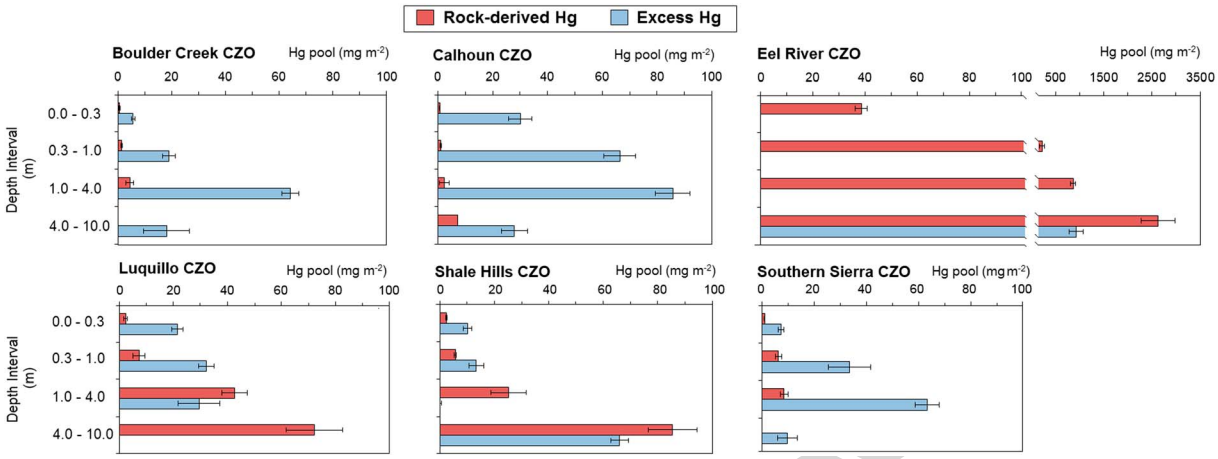

Figure 3. Mercury inventories for the four depth intervals of the six Critical Zone Observatories (CZOs). The $Hg_{rock\text{-}derived}$ and Hg_{excess} values were calculated using equation (1) and converted to areal units using bulk density and sample depths. Error bars are cumulative standard error for Hg concentrations and bulk density measurements.

4. Discussion

4.1. Mercury Concentrations and Inventories in Weathering Profiles

Hg concentrations across the six weathering profiles (0.4 to 282 ng/g) were comparable to the range of values reported by previous studies on nonpoint source polluted forested soils in North America (e.g., Obrist et al., 2009; Obrist et al., 2011; Richardson et al., 2013; Richardson & Friedland, 2015; Smith et al., 2013), tropical South America (e.g., Fiorentino et al., 2011), temperate and subtropical China (Luo et al., 2014), and temperate and Mediterranean Europe (Peña-Rodríguez et al., 2012; Schwesig & Matzner, 2001). Furthermore, Hg concentrations were generally lower than those reported in point-source polluted areas such as soils near artisanal gold mining (e.g., 70–420 ng/g of soils in French Guyana studied by Guedron et al., 2009) and soils near metropolitan areas in China (e.g., 110–2178 ng/g in Shi et al., 2013). The spatial variation in Hg_{excess} among CZOs was generally in agreement with Smith-Downey et al. (2010), which estimated higher anthropogenic enrichment in surface soils in the eastern United States and at higher elevations. These results agree with atmospheric deposition models that estimate higher Hg concentrations near geologic sources along the Pacific coast in California and high atmospheric deposition rates to the eastern United States (Obrist et al., 2011; Smith et al., 2013; Smith-Downey et al., 2010).

Elevated Hg concentrations in soils extend far beyond the typical maximum sampling depth of 0.3 or even 0.5 m (Figure 1). Moreover, estimates for Hg inventories in the top 0.3 m and top 1.0 m of regolith were much higher in our study than Smith-Downey et al. (2010). Smith-Downey et al. (2010) estimated that Hg storage in soils in North America was typically between 1 and 10 mg/m^2 for the top 0.3 m, but our study estimated Hg storage in the top 0.3 m, which ranged from 6 to 30 mg/m^2. Furthermore, as shown in Figures 1, 2, and 3, the accumulation of Hg in regolith extends far deeper into the weathering profile and indicates deeper Hg inventories. For Boulder Creek, Calhoun, and Southern Sierra CZOs, Hg_{excess} was a dominant portion of the Hg concentrations and bulk regolith inventories (Figures 2 and 3). Further, Hg_{excess} inventories from the 0.3–1.0-, 1.0–4.0-, and 4.0–10.0-m depth intervals were equal to, or larger than, the Hg_{excess} inventory in the top 0–0.3 m. These results highlight that substantial Hg can be sequestered within regolith, deeper in the weathering profile than commonly sampled. Because large portions of the Hg inventories were estimated to not be sourced from weathering within the profile on the basis of Hg_{excess} values, we suggest that regolith deeper than 0.3 or 0.5 m is integral in mediating Hg sequestration from the atmosphere.

We calculated that the 0–10 m of regolith had accumulated 90–860 mg/m^2 of Hg_{excess}, up to two orders of magnitude greater Hg inventories than in Smith-Downey et al. (2010). This unaccounted Hg

Table 2
R Values for Linear Relationships Between Mercury and Total Organic Carbon

Study area	Total Hg	Hg_{excess}	$Hg_{rock\text{-}derived}$
Boulder Creek CZO	0.34	0.34	0.02
Calhoun CZO	−0.23	−0.23	0.47
Eel River CZO	−0.02	0.30	−0.31
Luquillo CZO	0.91**	0.92**	−0.63*
Shale Hills CZO	0.96**	0.97**	0.24
Southern Sierra CZO	0.48	0.48	0.46

Note. Significant linear regressions are denoted with * for $p < 0.05$ and ** for $p < 0.01$.

could be active in the global Hg cycle interacting with the atmosphere, oceans, and terrestrial systems or sequestered away as part of the deep mineral reservoir. Incorporating deeper regolith Hg is difficult because estimating the extent of Hg accumulation and its rate of Hg sequestration are unclear and require additional data. First, extrapolating Hg in regolith is difficult as estimating the thickness of regolith across North America has been limited. Regolith can range between 3 and 40 m with strong variations with lithology, petrology, topography, and climate (Bazilevskaya et al., 2012; Holbrook et al., 2014; St. Clair et al., 2015). Pelletier et al. (2016) developed a physically based model to estimate soil thickness across the United States and estimated the average soil and regolith thickness to be approximately 6 m, although this is a key resource exploring the role of regolith. Second, the rate of Hg accumulation in regolith is not constant and has varied over recent and geologic timescales. Based upon total human Hg emission estimates from Streets et al. (2017), it can be presumed that the much larger Hg inventories in regolith across these six CZOs have been accumulating on the geologic timescale of kyr to Myr and are likely not primarily from the recent spike in anthropogenic Hg deposition over the past century and a half. However, that is not to understate that anthropogenic pressures (e.g., land-use change and erosion) are not capable of mobilizing these inventories into the global Hg system. Biogeochemists who study Hg must excavate deeper, and modelers must begin to consider deep sequestration of Hg in the regolith.

Our results suggest that regolith, beyond surface soils, can be a large net sink for Hg or potentially a net source. Hg_{excess} concentrations and inventories at Boulder Creek, Calhoun, and Southern Sierra CZOs show that regolith acts as a sink throughout the weathering profile for Hg not sourced from the weathering of parent materials, although the provenance of the Hg_{excess} is unclear. We hypothesize that much of the Hg_{excess} was sourced from atmospheric deposition or lateral transport from geologic sources over kyr to Myr timescales. Since regolith samples are from upland sites and not topographic low points on their respective landscapes, we suggest the influence of lateral transport to be minimal and atmospheric deposition to be a dominant source for Hg_{excess}. In addition, lateral transport into the regolith profile would likely be balanced by lateral transport out of the regolith profile. However, vertical transport of Hg within the profile may be important, especially at Calhoun CZO, Eel River CZO, and Luquillo CZO due to their subsurface Hg_{excess} concentration peaks.

Based upon cumulative estimates of Hg, additions from human deposition from Smith-Downey et al. (2010) ranged between 0.1 and 1 mg/m^2 cumulative while excess Hg inventories in our study ranged between 106 and 860 mg/m^2 in the top 10 m of regolith profiles. Thus, only surface soils have been influenced by anthropogenic emissions since industrialization (Amos et al., 2013; Streets et al., 2017). Moreover, anthropogenic Hg is most likely sequestered primarily in surface soils due to the strong sorption to organic C (Obrist et al., 2011; Shi et al., 2013). Thus, we attribute the majority of Hg_{excess} directly to atmospheric Hg sources from volcanic emissions and emission and resuspension from terrestrial and marine sources over geologic timescale of kyr to Myr. In addition, regolith may have also accumulated Hg from lateral transport and leaching from other depths within each weathering profile, particularly at Eel River CZO due to its high $Hg_{rock\text{-}derived}$ concentration.

Hg concentrations and inventories in regolith at the tropical, highly weathered Luquillo, and the sedimentary-dominated Eel River, and Shale Hills CZOs were dominated by $Hg_{rock\text{-}derived}$ for two distinct reasons. Luquillo CZO is dominated by igneous-derived regolith that has low Hg concentrations but does not appear to act as a Hg sink as do the other igneous weathering profiles. Shanley et al. (2008) compared the Hg budget for the same watershed at Luquillo CZO to the Hg budgets in similar-sized watersheds in Colorado, Wisconsin, Georgia, and Vermont, USA, and found Luquillo to be a net source of Hg. As noted by Shanley et al. (2008), the Luquillo study site has a mean annual precipitation of 4,200 mm/year, while the other five study areas have mean annual precipitation values between 700 and 2,000 mm/year. Thus, greater movement of water could rapidly transport Hg bound to inorganic and TOC particulates through the regolith profile at rates that exceed their physical immobilization. Shanley et al. (2008) found that particulates of organic C were responsible for 93% of stream water export of Hg at Luquillo CZO compared to $<$65% at their four other studied watersheds. Moreover, soil erosion could also be responsible for the lower retention of Hg at Luquillo CZO (Larsen & Torres-Sánchez, 1998; Munthe & Hultberg, 2004). Hg in the weathering profiles at Eel River and Shale Hills CZOs were predominately $Hg_{rock\text{-}derived}$ because their sedimentary parent rock has higher Hg concentrations compared to igneous- and metamorphic-derived regolith. However, atmospheric

Hg deposition has likely influenced the surface soils at Shale Hills substantially because of upwind combustion of coal for energy production (Figure 2; e.g., Keeler et al., 2006).

A potential source of error with the Hg/Ti normalization is that Hg in bedrock exists in sulfide minerals while Ti is present in aluminosilicate minerals, and both may not be homogeneously distributed in the rocks and minerals of the regolith. This assumption would most likely underestimate HgS in regolith because of its wide variation in rocks relative to Ti (see Smith et al., 2008), leading to underestimation of $Hg_{rock\text{-}derived}$. Similarly, Ti may be mobile in the surface soil (<0.25 m) at the Luquillo CZO (Buss et al., 2017), meaning that Hg/Ti in the surface soils at Luquillo could be overestimated, causing an underestimation of $Hg_{rock\text{-}derived}$. This highlights the importance of choosing a representative value for the parent material Hg/Ti ratios as variations in bedrock Hg/Ti ratios can mask effects of weathering with depth, as present in Eel River CZO. Further, we believe our homogenization of rock samples aided in avoiding in the mineral Ti and Hg bias. Although these errors of heterogeneity and representative parent material samples exist, this method has been used in tandem with Hg deposition estimates to effectively predict Hg loadings in weathering profiles exposed to regional Hg deposition (e.g., Grimaldi et al., 2008; Guedron et al., 2006; Zhang et al., 2015).

4.2. Mercury, TOC, and Other Physicochemical Properties in Regolith

Hg concentrations in soil is generally related to chemical properties, specifically TOC concentrations, but other properties like clay abundance and secondary oxide abundance can also be key factors (e.g., Demers et al., 2013; Obrist et al., 2011; Richardson et al., 2013). Plant-derived organic C is a key soil property for Hg adsorption, and most studies on Hg in forest soils have observed a significant relationship between Hg and TOC. Using linear regressions for each CZO and a cross-CZO generalized linear mixed effect model, Hg concentrations throughout the weathering profile were significantly correlated with TOC only at Luquillo and Shale Hills CZOs (Table 2). Further, the significant relationship between TOC and Hg_{excess} for Luquillo and Shale Hills CZOs (Table 2) indicates that a large portion of Hg that accumulated in regolith from exogenous sources can be controlled by organic C cycling, as suggested by Obrist et al. (2011) and Smith-Downey et al. (2010). Overall, Hg concentrations were not significantly correlated with TOC across study areas using a generalized linear mixed-effects model with each CZO as a random effect variable. The overall lack of a strong relationship between Hg and C suggests that Hg sorption to organic C is dominant for some parts of the critical zone, but other processes control Hg accumulation in regolith.

We suggest that accumulations of clay minerals, Fe minerals (both oxyhydroxides and Fe(II) sulfide minerals), and hydrogeochemical processes controlling redox conditions and leaching rates are responsible for peaks in Hg accumulation at Southern Sierra, Luquillo, Boulder Creek CZOs, and most strikingly at Calhoun CZO (Richardson & Richter, 2017). Figure 1 shows that Hg concentrations deeper than 1.0 m match or exceed surface soil Hg concentrations at three of the four CZOs. Since many of these subsurface peaks do not coincide with higher TOC concentrations, we hypothesize that this indicates that processes other than sorption by organic C are influencing Hg accumulation in the weathering profile. At Calhoun and Luquillo CZOs, these elevated concentrations of Hg correspond with redoximorphic features of localized reduced and oxidized Fe. At Calhoun CZO, the higher Hg concentrations correspond with orange-gray bands (Richardson & Richter, 2017). The orange-gray bands are characterized by accumulations of hematite and goethite and gray bands are Fe depleted and composed of 73% clay-sized particles dominated by kaolinite and hydroxy-interlayered vermiculite with elevated organic C (Fimmen et al., 2008). Reduced Fe, clay minerals, and organic C are known to enhance sorption of Hg (Fiorentino et al., 2011; Gabriel & Williamson, 2004; Grimaldi et al., 2008). At Luquillo CZO, the subsurface Hg peak (~1.5 m depth) corresponded with a small spike in TOC, likely related to a hydrogeochemical process promoting subsurface organic C accumulation. These subsurface Hg accumulations demonstrate that only collecting shallow soil samples may overlook important deeper zones of Hg sequestration.

Our study has also shown that parent materials with elevated Hg concentrations can be net Hg sources with weathering extending >10.0 m in depth. Our results enabled us to attribute the majority of Hg in the weathering profile at Eel River and Shale Hills CZO to sedimentary parent material. We hypothesize that the elevated concentrations of Hg in the top 0.6 m at Shale Hills CZO are from regional atmospheric deposition (Figure 2), likely from regional industrial activities. However, the rest of the profile shows little sequestration of exogenously sourced Hg (Figure 2) and steady concentrations of Hg in the olive-pink, grayish-buff shale. An additional factor influencing Hg at Shale Hills is the relatively young weathering profile due to

periglacial conditions occurring during the last glacial maximum of approximately 15 kyr (Jin et al., 2011). Eel River CZO was also dominated by Hg sourced from weathering of sedimentary parent material, argillite (Smith et al., 2008). Subsurface peaks at 7.3 m suggested potential downward vertical transport of Hg within the profile or heterogeneity in bedrock. Thus, areas with fine-grained sedimentary rocks with elevated Hg concentrations may be important for regional Hg sources to aquatic ecosystems.

5. Conclusions and Implications for the Global Hg Biogeochemical Cycle

Sequestration of Hg in regolith well below surface soil, several meters in depth, has been underappreciated by most empirical and modeling studies on regional and global Hg cycling. Our results show that elevated Hg concentrations extend beyond the typical maximum sampling depth of 0.3 to 0.5 m. Surface soils (0–0.3 m) at each CZO except Shale Hills had Hg concentrations lower than or equal to subsurface peaks in regolith at the 1.5–8.0-m depth. One of the most important findings in our study was that Hg/Ti ratios suggest that total Hg concentrations and inventories were primarily Hg_{excess}, atmospherically derived not weathering sourced Hg, for three of the six weathering profiles. Our Hg profiles demonstrate that regolith below surface soils are sequestering Hg from external sources.

Considering Hg deeper in the weathering profile, >0.5 m in depth, in the global Hg biogeochemical cycle is essential as regolith has the potential to store up to two orders of magnitude more Hg than the top 0–0.3 m. Hg sequestration was associated with but not necessarily governed by organic C. Lithology clearly influences Hg concentrations as observed by the high rock-derived Hg from argillite at the Eel River CZO. Additional factors influencing Hg sequestration in regolith are clay abundance, Fe mineralogy, and hydrogeochemical processes, such as at the Luquillo CZO with potentially high leaching and erosion rates. Thus, we conclude that while linking the global Hg biogeochemical cycle directly to that of C has provided an excellent first-order approximation, it fails to account for inorganic processes occurring deeper in the weathering profile. Our findings highlight the importance of inorganic and geologic processes in the global Hg cycle.

The sequestration and sourcing of Hg in the Critical Zone have many implications for ecotoxicology and land-use considerations. First, identifying regolith and areas prone to Hg sourcing is important for protecting human and ecological health. For example, substantial Hg concentrations and methyl-Hg has been found in filtered water samples and algae in the South Fork Eel River where anthropogenic Hg pollution is insignificant (Tsui et al., 2010). Hg from regolith weathering can bioaccumulate in top trophic fish from insects in terrestrial ecosystems (Tsui et al., 2014). Second, determining areas of the Critical Zone that sequester large inventories of Hg could be important for protecting sensitive riparian and aquatic ecosystems. However, locating these regions and their stability under different land uses requires further investigation (e.g., Almeida et al., 2005; Chen et al., 2010; Cordeiro et al., 2002; Richardson et al., 2017).

Acknowledgments
This work was made possible by the National Science Foundation grant (NSF-1360760) to the Critical Zone Observatory Network National Office. Funding from the National Science Foundation for each CZO was also instrumental in this project: Boulder Creek (NSF-1331828), Calhoun (NSF-1331846), Eel River (NSF-1331940), Luquillo (NSF-1331841), Shale Hills (NSF-1331726), and Southern Sierra (NSF-1331939). The authors are thankful for the help with obtaining samples from Erin Stacy (UC Merced), Stephen Hart (UC Merced), Scott Hynek (Penn State), Sue Brantley (Penn State), and Andy Kurtz (Boston University). We are thankful for the UC Angelo Coast Range Reserve and the analytical help from Brian Jackson (Dartmouth College) and Mary Catherine Reinthal (Cornell). Mercury concentration and inventory data are available in the supporting information.

References

Almeida, M. D., Lacerda, L. D., Bastos, W. R., & Herrmann, J. C. (2005). Mercury loss from soils following conversion from forest to pasture in Rondônia, Western Amazon, Brazil. *Environmental Pollution*, *137*(2), 179–186. https://doi.org/10.1016/j.envpol.2005.02.026

Amos, H. M., Jacob, D. J., Streets, D. G., & Sunderland, E. M. (2013). Legacy impacts of all-time anthropogenic emissions on the global mercury cycle. *Global Biogeochemical Cycles*, *27*, 410–421. https://doi.org/10.1002/gbc.20040

Andren, A. W., & Nriagu, J. O. (1979). The global cycle of mercury. *Biogeochemistry of Mercury in the Environment*, 1–15. Q9

Bacon, A. R., Richter, D. D., Bierman, P. R., & Rood, D. H. (2012). Coupling meteoric ^{10}Be with pedogenic losses of ^{9}Be to improve soil residence time estimates on an ancient North American interfluve. *Geology*, *40*(9), 847–850. https://doi.org/10.1130/G33449.1

Bloom, N. S. (1992). On the chemical form of mercury in edible fish and marine invertebrate tissue. *Canadian Journal of Fisheries and Aquatic Sciences*, *49*(5), 1010–1017. https://doi.org/10.1139/f92-113

Brimhall, G. H., & Dietrich, W. E. (1987). Constitutive mass balance relations between chemical composition, volume, density, porosity, and strain in metasomatic hydrochemical systems: Results on weathering and pedogenesis. *Geochimica et Cosmochimica Acta*, *51*(3), 567–587. https://doi.org/10.1016/0016-7037(87)90070-6

Buss, H. L., Bruns, M. A., Schultz, M. J., Moore, J., Mathur, C. F., & Brantley, S. L. (2005). The coupling of biological iron cycling and mineral weathering during saprolite formation, Luquillo Mountains, Puerto Rico. *Geobiology*, *3*(4), 247–260. https://doi.org/10.1111/j.1472-4669.2006.00058.x

Buss, H. L., Lara, M. C., Moore, O. W., Kurtz, A. C., Schulz, M. S., & White, A. F. (2017). Lithological influences on contemporary and long-term regolith weathering at the Luquillo Critical Zone Observatory. *Geochimica et Cosmochimica Acta*, *196*, 224–251. https://doi.org/10.1016/j.gca.2016.09.038

Buss, H. L., & White, A. F. (2012). Weathering processes in the Icacos and Mameyes watersheds in eastern Puerto Rico. In S. F. Murphy, & R. F. Stallard (Eds.), *Water quality and landscape processes of four watersheds in eastern Puerto Rico*, *US Geological Survey Professional Paper*, (Vol. 1789, pp. 249–262). Reston, VA: U.S. Department of the Interior, U.S. Geological Survey.

Chen, X., Xia, X., Wu, S., Wang, F., & Guo, X. (2010). Mercury in urban soils with various types of land use in Beijing, China. *Environmental Pollution*, *158*(1), 48–54. https://doi.org/10.1016/j.envpol.2009.08.028

Cordeiro, R. C., Turcq, B., Ribeiro, M. G., Lacerda, L. D., Capitaneo, J., da Silva, A. O., et al. (2002). Forest fire indicators and mercury deposition in an intense land use change region in the Brazilian Amazon (Alta Floresta, MT). *Science of the Total Environment*, *293*(1-3), 247–256. https://doi.org/10.1016/S0048-9697(02)00045-1

Demers, J. D., Yavitt, J. B., Driscoll, C. T., & Montesdeoca, M. R. (2013). Legacy mercury and stoichiometry with C, N, and S in soil, pore water, and stream water across the upland-wetland interface: The influence of hydrogeologic setting. *Journal of Geophysical Research: Biogeosciences*, *118*, 825–841. https://doi.org/10.1002/jgrg.20066

Driscoll, C. T., Han, Y. J., Chen, C. Y., Evers, D. C., Lambert, K. F., Holsen, T. M., et al. (2007). Mercury contamination in forest and freshwater ecosystems in the northeastern United States. *Bioscience*, *57*(1), 17–28. https://doi.org/10.1641/B570106

Driscoll, C. T., Mason, R. P., Chan, H. M., Jacob, D. J., & Pirrone, N. (2013). Mercury as a global pollutant: Sources, pathways, and effects. *Environmental Science & Technology*, *47*(10), 4967–4983. https://doi.org/10.1021/es305071v

Druhan, J. L., Fernandez, N., Wang, J., Dietrich, W. E., & Rempe, D. (2017). Seasonal shifts in the solute ion ratios of vadose zone rock moisture from the Eel River Critical Zone Observatory. *Acta Geochimica*, *36*(3), 385–388. https://doi.org/10.1007/s11631-017-0169-z

Fimmen, R. L., Vasudevan, D., Williams, M. A., & West, L. T. (2008). Rhizogenic Fe–C redox cycling: A hypothetical biogeochemical mechanism that drives crustal weathering in upland soils. *Biogeochemistry*, *87*(2), 127–141. https://doi.org/10.1007/s10533-007-9172-5

Fiorentino, J. C., Enzweiler, J., & Angélica, R. S. (2011). Geochemistry of mercury along a soil profile compared to other elements and to the parental rock: Evidence of external input. *Water, Air, & Soil Pollution*, *221*(1-4), 63–75. https://doi.org/10.1007/s11270-011-0769-x

Fuller, T. K., Perg, L. A., Willenbring, J. K., & Lepper, K. (2009). Field evidence for climate-driven changes in sediment supply leading to strath terrace formation. *Geology*, *37*(5), 467–470. https://doi.org/10.1130/G25487A.1

Gabriel, M. C., & Williamson, D. G. (2004). Principal biogeochemical factors affecting the speciation and transport of mercury through the terrestrial environment. *Environmental Geochemistry and Health*, *26*(3-4), 421–434. https://doi.org/10.1007/s10653-004-1308-0

Garcia-Martino, A., Warner, G., Scatena, F., & Civco, D. (1996). Rainfall, runoff and elevation relationships in the Luquillo Mountains of Puerto Rico. *Caribbean Journal of Science*, *32*, 413–424.

Grimaldi, C., Grimaldi, M., & Guedron, S. (2008). Mercury distribution in tropical soil profiles related to origin of mercury and soil processes. *Science of the Total Environment*, *401*(1-3), 121–129. https://doi.org/10.1016/j.scitotenv.2008.04.001

Guedron, S., Grangeon, S., Lanson, B., & Grimaldi, M. (2009). Mercury speciation in a tropical soil association; Consequence of gold mining on Hg distribution in French Guiana. *Geoderma*, *153*(3-4), 331–346. https://doi.org/10.1016/j.geoderma.2009.08.017

Guedron, S., Grimaldi, C., Chauvel, C., Spadini, L., & Grimaldi, M. (2006). Weathering versus atmospheric contributions to mercury concentrations in French Guiana soils. *Applied Geochemistry*, *21*(11), 2010–2022. https://doi.org/10.1016/j.apgeochem.2006.08.011

Harris, H. H., Pickering, I. J., & George, G. N. (2003). The chemical form of mercury in fish. *Science*, *301*(5637), 1203–1203. https://doi.org/10.1126/science.1085941

Hissler, C., & Probst, J. L. (2006). Impact of mercury atmospheric deposition on soils and streams in a mountainous catchment (Vosges, France) polluted by chlor-alkali industrial activity: The important trapping role of the organic matter. *Science of the Total Environment*, *361*(1-3), 163–178. https://doi.org/10.1016/j.scitotenv.2005.05.023

Hojdová, M., Rohovec, J., Chrastný, V., Penížek, V., & Navrátil, T. (2015). The influence of sample drying procedures on mercury concentrations analyzed in soils. *Bulletin of Environmental Contamination and Toxicology*, *94*(5), 570–576. https://doi.org/10.1007/s00128-015-1521-9

Holbrook, W. S., Riebe, C. S., Elwaseif, M., Hayes, J. L., Basler-Reeder, K., Harry, D. L., et al. (2014). Geophysical constraints on deep weathering and water storage potential in the Southern Sierra Critical Zone Observatory. *Earth Surface Processes and Landforms*, *39*(3), 366–380. https://doi.org/10.1002/esp.3502

Holmes, P., James, K. A. F., & Levy, L. S. (2009). Is low-level environmental mercury exposure of concern to human health? *Science of the Total Environment*, *408*(2), 171–182. https://doi.org/10.1016/j.scitotenv.2009.09.043

Hunsaker C. T., & Eagan, S. M. (2003). Small stream ecosystem variability in the Sierra Nevada of California. In K.G. Renard (ed.) *First interagency conference on research in the watersheds*. 27–30 Oct. 2003. USDA-ARS, Washington, DC. 716–721. Q10

Hylander, L. D., & Meili, M. (2003). 500 years of mercury production: Global annual inventory by region until 2000 and associated emissions. *Science of the Total Environment*, *304*(1-3), 13–27. https://doi.org/10.1016/S0048-9697(02)00553-3

Jin, L., Andrews, D. M., Holmes, G. H., Lin, H., & Brantley, S. L. (2011). Opening the "black box": Water chemistry reveals hydrological controls on weathering in the Susquehanna Shale Hills Critical Zone Observatory. *Vadose Zone Journal*, *10*(3), 928–942. https://doi.org/10.2136/vzj2010.0133

Jin, L., Ravella, R., Ketchum, B., Bierman, P. R., Heaney, P., White, T., & Brantley, S. L. (2010). Mineral weathering and elemental transport during hillslope evolution at the Susquehanna/Shale Hills Critical Zone Observatory. *Geochimica et Cosmochimica Acta*, *74*(13), 3669–3691. https://doi.org/10.1016/j.gca.2010.03.036

Keeler, G. J., Landis, M. S., Norris, G. A., Christianson, E. M., & Dvonch, J. T. (2006). Sources of mercury wet deposition in eastern Ohio, USA. *Environmental Science & Technology*, *40*(19), 5874–5881. https://doi.org/10.1021/es060377q

Lamborg, C. H., Fitzgerald, W. F., O'Donnell, J., & Torgersen, T. (2002). A non-steady-state compartmental model of global-scale mercury biogeochemistry with interhemispheric atmospheric gradients. *Geochimica et Cosmochimica Acta*, *66*(7), 1105–1118. https://doi.org/10.1016/S0016-7037(01)00841-9

Larsen, M. C., & Torres-Sánchez, A. J. (1998). The frequency and distribution of recent landslides in three montane tropical regions of Puerto Rico. *Geomorphology*, *24*, 309–331.

Luo, Y., Duan, L., Wang, L., Xu, G., Wang, S., & Hao, J. (2014). Mercury concentrations in forest soils and stream waters in northeast and south China. *Science of the Total Environment*, *496*, 714–720. https://doi.org/10.1016/j.scitotenv.2014.07.036

Melgar, M. J., Alonso, J., & García, M. A. (2009). Mercury in edible mushrooms and underlying soil: Bioconcentration factors and toxicological risk. *Science of the Total Environment*, *407*(20), 5328–5334. https://doi.org/10.1016/j.scitotenv.2009.07.001

Munthe, J., & Hultberg, H. (2004). Mercury and methylmercury in runoff from a forested catchment—Concentration, fluxes, and their response to manipulations. *Water, Air, & Soil Pollution: Focus*, *4*(2/3), 607–618. https://doi.org/10.1023/B:WAFO.0000028381.04393.ed

Murphy, S. F., Stallard, R. F., Larsen, M. C., & Gould, W. A. (2012). Physiography, geology, and land cover of four watersheds in eastern Puerto Rico. In S. F. Murphy, & R. F. Stallard (Eds.), *Water quality and landscape processes of four watersheds in eastern Puerto Rico*, *US Geological Survey Professional Paper*, (Vol. 1789, pp. 1–23). Reston, VA: U.S. Department of the Interior, U.S. Geological Survey.

Murphy, S. F., Stallard, R. F., Scholl, M. A., González, G., & Torres-Sánchez, A. J. (2017). Reassessing rainfall in the Luquillo Mountains, Puerto Rico: Local and global ecohydrological implications. *PLoS One*, *12*(7), e0180987. https://doi.org/10.1371/journal.pone.0180987

Nriagu, J., & Becker, C. (2003). Volcanic emissions of mercury to the atmosphere: Global and regional inventories. *Science of the Total Environment*, *304*(1-3), 3–12. https://doi.org/10.1016/S0048-9697(02)00552-1

Obrist, D., Johnson, D. W., & Lindberg, S. E. (2009). Mercury concentrations and pools in four Sierra Nevada forest sites, and relationships to organic carbon and nitrogen. *Biogeosciences*, *6*(5), 765–777. https://doi.org/10.5194/bg-6-765-2009

Obrist, D., Johnson, D. W., Lindberg, S. E., Luo, Y., Hararuk, O., Bracho, R., et al. (2011). Mercury distribution across 14 U.S. forests. Part 1: Spatial patterns of concentrations in biomass, litter, and soils. *Environmental Science and Technology*, *45*(9), 3974–3981. https://doi.org/10.1021/es104384m

Oh, N. H., & Richter, D. D. (2005). Elemental translocation and loss from three highly weathered soil–bedrock profiles in the southeastern United States. *Geoderma*, *126*(1-2), 5–25. https://doi.org/10.1016/j.geoderma.2004.11.005

Orlando, J., Comas, X., Hynek, S. A., Buss, H. L., & Brantley, S. L. (2016). Architecture of the deep critical zone in the Río Icacos watershed (Luquillo Critical Zone Observatory, Puerto Rico) inferred from drilling and ground penetrating radar (GPR). *Earth Surface Processes and Landforms*, *41*(13), 1826–1840. https://doi.org/10.1002/esp.3948

Pelletier, J. D., Broxton, P. D., Hazenberg, P., Zeng, X., Troch, P. A., Niu, G. Y., et al. (2016). A gridded global data set of soil, intact regolith, and sedimentary deposit thicknesses for regional and global land surface modeling. *Journal of Advances in Modeling Earth Systems*, *8*(1), 41–65 . https://doi.org/10.1002/2015MS000526

Peña-Rodríguez, S., Pontevedra-Pombal, X., Fernández-Calviño, D., Taboada, T., Arias-Estévez, M., Martínez-Cortizas, A., et al. (2012). Mercury content in volcanic soils across Europe and its relationship with soil properties. *Journal of Soils and Sediments*, *12*(4), 542–555. https://doi.org/10.1007/s11368-011-0468-7

Pirrone, N., Cinnirella, S., Feng, X., Finkelman, R. B., Friedli, H. R., Leaner, J., et al. (2009). *Global mercury emissions to the atmosphere from natural and anthropogenic sources*, (pp. 3–49). New York, USA, Chap. 1: Springer.

Richardson, J. B., & Friedland, A. J. (2015). Mercury in coniferous and deciduous upland forests in northern New England, USA: Implications of climate change. *Biogeosciences*, *12*(22), 6737–6749. https://doi.org/10.5194/bg-12-6737-2015

Richardson, J. B., Friedland, A. J., Engerbretson, T. R., Kaste, J. M., & Jackson, B. P. (2013). Spatial and vertical distribution of mercury in upland forest soils across the northeastern United States. *Environmental Pollution*, *182*, 127–134. https://doi.org/10.1016/j.envpol.2013.07.011

Richardson, J. B., Görres, J. H., Jackson, B. P., & Friedland, A. J. (2015). Trace metals and metalloids in forest soils and exotic earthworms in northern New England, USA. *Soil Biology and Biochemistry*, *85*, 190–198. https://doi.org/10.1016/j.soilbio.2015.03.001

Richardson, J. B., Petrenko, C. L., & Friedland, A. J. (2017). Organic horizon and mineral soil mercury along three clear-cut forest chronosequences across the northeastern USA. *Environmental Science and Pollution Research*, *24*(36), 27994–28005. https://doi.org/10.1007/s11356-017-0356-9

Richardson, J. B., & Richter, D. D. (2017). Mercury in soils of the Calhoun Critical Zone Observatory: Importance of redox features in sequestration. Paper presented at 2017 Annual Meeting of the Soil Science Society of America, Tampa, Florida.

Richter, D. D. Jr., & Markewitz, D. (2001). *Understanding soil change: soil sustainability over millennia, centuries, and decades*. Cambridge, UK: Cambridge University Press.

Rimmer, C. C., McFarland, K. P., Evers, D. C., Miller, E. K., Aubry, Y., Busby, D., & Taylor, R. J. (2005). Mercury concentrations in Bicknell's thrush and other insectivorous passerines in montane forests of northeastern North America. *Ecotoxicology*, *14*(1-2), 223–240. https://doi.org/10.1007/s10646-004-6270-1

Roulet, M., Lucotte, M., Saint-Aubin, A., Tran, S., Rheault, I., Farella, N., et al. (1998). The geochemistry of mercury in central Amazonian soils developed on the Alter-do-Chao formation of the lower Tapajos River Valley, Para state, Brazil. *Science of the Total Environment*, *223*(1), 1–24. https://doi.org/10.1016/S0048-9697(98)00265-4

Schuster, P. F., Schaefer, K. M., Aiken, G. R., Antweiler, R. C., Dewild, J. F., Gryziec, J. D., et al. (2018). Permafrost stores a globally significant amount of mercury. *Geophysical Research Letters*, *45*, 1463–1471. https://doi.org/10.1002/2017GL075571

Schwesig, D., & Matzner, E. (2001). Dynamics of mercury and methylmercury in forest floor and runoff of a forested watershed in Central Europe. *Biogeochemistry*, *53*(2), 181–200. https://doi.org/10.1023/A:1010600600099

Selin, N. E. (2009). Global biogeochemical cycling of mercury: A review. *Annual Review of Environment and Resources*, *34*(1), 43–63. https://doi.org/10.1146/annurev.environ.051308.084314

Shanley, J. B., Mast, M. A., Campbell, D. H., Aiken, G. R., Krabbenhoft, D. P., Hunt, R. J., et al. (2008). Comparison of total mercury and methylmercury cycling at five sites using the small watershed approach. *Environmental Pollution*, *154*(1), 143–154. https://doi.org/10.1016/j.envpol.2007.12.031

Shi, J. B., Meng, M., Shao, J. J., Zhang, K. G., Zhang, Q. H., & Jiang, G. B. (2013). Spatial distribution of mercury in topsoil from five regions of China. *Environmental Science and Pollution Research*, *20*(3), 1756–1761. https://doi.org/10.1007/s11356-012-1115-6

Smith, C. N., Kesler, S. E., Blum, J. D., & Rytuba, J. J. (2008). Isotope geochemistry of mercury in source rocks, mineral deposits and spring deposits of the California Coast Ranges, USA. *Earth and Planetary Science Letters*, *269*(3-4), 399–407. https://doi.org/10.1016/j.epsl.2008.02.029

Smith, D. B., Cannon, W. F., Woodruff, L. G., Solano, F., Kilburn, J. E., & Fey, D. L. (2013). Geochemical and mineralogical data for soils of the conterminous United States. *US Geological Survey Data Series*, *801*, 19.

Smith-Downey, N. V., underland, E. M., & Jacob, D. J. (2010). Anthropogenic impacts on global storage and emissions of mercury from terrestrial soils: Insights from a new global model. *Journal of Geophysical Research*, *115*, G03008. https://doi.org/10.1029/2009JG001124

Streets, D. G., Horowitz, H. M., Jacob, D. J., Lu, Z., Levin, L., Ter Schure, A. F., & Sunderland, E. M. (2017). Total mercury released to the environment by human activities. *Environmental Science & Technology*, *51*(11), 5969–5977. https://doi.org/10.1021/acs.est.7b00451

Sullivan, P. L., Hynek, S. A., Gu, X., Singha, K., White, T., West, N., et al. (2016). Oxidative dissolution under the channel leads geomorphological evolution at the Shale Hills catchment. *American Journal of Science*, *316*(10), 981–1026. https://doi.org/10.2475/10.2016.02

Tsui, M. T. K., Blum, J. D., Finlay, J. C., Balogh, S. J., Nollet, Y. H., Palen, W. J., & Power, M. E. (2014). Variation in terrestrial and aquatic sources of methylmercury in stream predators as revealed by stable mercury isotopes. *Environmental Science & Technology*, *48*(17), 10128–10135. https://doi.org/10.1021/es500517s

Tsui, M. T. K., Finlay, J. C., Balogh, S. J., & Nollet, Y. H. (2010). In situ production of methylmercury within a stream channel in northern California. *Environmental Science & Technology*, *44*(18), 6998–7004. https://doi.org/10.1021/es101374y

Wang, S., Xing, D., Wei, Z., & Jia, Y. (2013). Spatial and seasonal variations in soil and river water mercury in a boreal forest, Changbai Mountain, northeastern China. *Geoderma*, *206*, 123–132. https://doi.org/10.1016/j.geoderma.2013.04.026 Q11

Weaver, P. L., & Gould, W. A. (2013). Forest vegetation along environmental gradients in northeastern Puerto Rico. In G. González, M. R. Willig, & R. B. Waide (Eds.), *Ecological gradient analyses in a tropical landscape*, *Ecological Bulletins*, (Vol. 54, pp. 43–66). Hoboken, NJ: Wiley-Blackwell.

White, A. F., Blum, A. E., Schulz, M. S., Vivit, D. V., Stonestrom, D. A., Larsen, M., et al. (1998). Chemical weathering in a tropical watershed, Luquillo Mountains, Puerto Rico: I. Long-term versus short-term weathering fluxes. *Geochimica et Cosmochimica Acta*, *62*(2), 209–226. https://doi.org/10.1016/S0016-7037(97)00335-9

Yu, X., Driscoll, C. T., Warby, R. A., Montesdeoca, M., & Johnson, C. E. (2014). Soil mercury and its response to atmospheric mercury deposition across the northeastern United States. *Ecological Applications*, *24*(4), 812–822. https://doi.org/10.1890/13-0212.1

Zahir, F., Rizwi, S. J., Haq, S. K., & Khan, R. H. (2005). Low dose mercury toxicity and human health. *Environmental Toxicology and Pharmacology*, *20*(2), 351–360. https://doi.org/10.1016/j.etap.2005.03.007

Zhang, H., Li, Y., Luo, Y., & Christie, P. (2015). Anthropogenic mercury sequestration in different soil types on the southeast coast of China. *Journal of Soils and Sediments*, *15*(4), 962–971. https://doi.org/10.1007/s11368-015-1062-1